

The effect of strain heterogeneity on the work hardening of polycrystals predicted by mean-field approaches

O. Castelnau^{a,*}, R. Brenner^a, R.A. Lebensohn^b

^a *Laboratoire des Propriétés Mécaniques et Thermodynamiques des Matériaux, CNRS, Université Paris Nord, 93430 Villetaneuse, France*

^b *Materials Science and Technology Division, Los Alamos National Laboratory, NM 87815, USA*

Received 22 September 2005; received in revised form 20 January 2006; accepted 11 February 2006

Available online 17 April 2006

Abstract

In polycrystalline aggregates deforming by crystal plasticity, the local shears on each slip system can be significantly affected by the intergranular interaction. Therefore, in the framework of mean-field approaches, the intragrain strain heterogeneity must be taken into account when dealing with microstructure evolution associated with strain hardening. For that goal, a novel treatment is proposed and applied to a two-dimensional linearly viscous polycrystal. The results of the implementation of this new hardening treatment within the self-consistent scheme are compared to those of a fast Fourier transform-based full-field computation, considered as a reference solution. It is shown that the evolution with strain of the grain average reference resolved shear stress (RRSS) is well reproduced by the proposed scheme. The overall stress response of the polycrystal is slightly underestimated, due to some intrinsic heterogeneity of the distribution of RRSS.

© 2006 Acta Materialia Inc. Published by Elsevier Ltd. All rights reserved.

Keywords: Work hardening; Polycrystal; Micromechanical modeling; Plastic deformation; Strain heterogeneity

1. Introduction

This paper is concerned with the way in which work hardening is introduced and estimated in the context of statistical homogenization methods for plastically deforming polycrystals. This important aspect of microstructural evolution results from the interactions between dislocations and obstacles (i.e. precipitates, dislocation structures, grain boundaries, etc.) and leads to a progressive increase of the resistance to dislocation motion by slip.

Since the pioneering experimental investigations of Taylor and Elam [1], numerous models have been proposed to describe the strain-hardening kinetics and anisotropy for different crystalline structures. A fundamental aspect of work hardening is related to the interaction between the different slip systems. In the theoretical formulation given

by Mandel [2] and Hill [3], the time derivative of the local reference resolved shear stress (RRSS) of a particular slip system k is linked to the local shear rates on every slip system k' through a local hardening matrix $h_{kk'}$. In general, the components of $h_{kk'}$ have a nonlinear dependence on the accumulated strain. Several forms for the hardening matrix have been proposed. Unlike Taylor's early assumption [4] of equality between all the components of $h_{kk'}$, subsequent experimental analyses have shown that the hardening is in essence anisotropic [5–8]. Several semi-empirical models have been developed to address the question of hardening kinetics. Besides a simple linear evolution law (constant $h_{kk'}$), saturating (or, at least, nonlinear) hardening arises from the competition between the processes of storage and annihilation of dislocations. This has been considered in two ways. On the one hand, several “mechanical” approaches using the accumulated slip and the RRSS on each system as internal variables have been proposed (e.g. Refs. [9–11]). On the other hand, several other “physically-based” hardening theories have been developed

* Corresponding author. Tel.: +33 01 49 40 34 68; fax: +33 01 49 40 39 38.

E-mail address: oc@lpmtm.univ-paris13.fr (O. Castelnau).

[12–15] using the dislocation densities on each system as internal variables, which are believed to be more closely linked to real microstructure evolution. Finally, it is also worth mentioning recent approaches based on an explicit scale transition from the dislocation structure to the single crystal [16,17].

The different forms of the work-hardening laws have been widely used within finite element (FE) simulations of the plastic response of single crystals [18,19], multicrystals [13,20,21] and polycrystals [22,23]. In Ref. [24] the overall hardening (i.e. the strain hardening due to dislocation interactions, and the geometric hardening induced by texture evolution) predicted by FE simulations was compared to the corresponding predictions of the simple upper-bound (Taylor) and lower-bound (Sachs) mean-field approaches. Since these FE computations were based on a discrete representation of the microstructure, they allowed one, for the first time, to discuss the differences between full-field and mean-field approaches in terms of the predicted strain heterogeneities, crystallographic texture, overall stress–strain behavior, etc.

As a matter of fact, due to the random character of the microstructure of polycrystals, mean-field approaches are particularly well adapted to polycrystalline aggregates. In this context, hardening laws of the type discussed above have been widely used to describe the microstructural evolution of polycrystals in a statistical way, either with the simple Taylor model [25,26] or with different nonlinear extensions of the self-consistent (SC) scheme (e.g. Refs. [27–34]). However, in concerning the latter SC formulations, it seems that some basic difficulties have been ignored up to now. The SC model has often been described as if each grain of the polycrystal would be treated as an ellipsoidal inclusion in a homogeneous matrix, leading to uniform stress and strain (rate) fields inside each grain. This simplified description is now known to be incorrect (e.g. Ref. [35]). From the determination of the intraphase variance of the mechanical fields, it has been shown that, at the scale of a “mechanical phase” (i.e. the set of grains of a polycrystal having the same orientation but different environments), a vanishing average slip rate does not mean a vanishing local slip rate [36]. Consequently, the local hardening law must be somehow averaged before being applied at the scale of a mechanical phase.

In connection with the above remarks, the main goal of the present article is to propose an improved way of introducing strain hardening in the context of mean-field approaches, accounting for the plastic slip heterogeneity at the level of a mechanical phase. Such treatment is necessary to improve the results of different practical applications of these widely used statistical methods for polycrystals. To start with, an improved hardening model will allow a more meaningful comparison and cross-validation between full-field and mean-field approaches (e.g. Refs. [37–39]). Also, the fitting procedure usually carried out in order to reproduce the stress–strain behavior of polycrystalline samples deformed along a given strain path,

and in turn used to predict the mechanical response of the same material along different strain paths (e.g. Ref. [40]), should provide a more general and accurate description of the material behavior if an improved hardening law is utilized. Finally, it is worth mentioning that when the behavior of two-phase polycrystals is modeled using the adjusted mechanical response of each constituent (e.g. Ref. [41]), the use of a hardening model sensitive to intra-phase heterogeneity should also contribute to improve the description of the mechanical behavior of such two-phase aggregates.

It should be emphasized that, while only very simple hardening models will be treated here (i.e. linear hardening), the proposed procedure can be extended without major difficulties to more general hardening laws. It is also worth noting that the present work is limited to linearly viscous polycrystals. This choice has to be made since all the existing nonlinear SC models are approximations based on different linearization schemes that essentially reduce the problem to the linear SC solution. Then, given that the results of these different nonlinear SC approximations are strongly dependent on the linearization scheme used, their comparison to any reference solution would become a difficult task. Therefore, the linear case has been preferred for the present study, based on which the more general case of nonlinear viscoplastic polycrystals will be treated and reported in the future.

For validation of the proposed model, its predictions will be compared with analogous results obtained by means of a full-field method based on the fast Fourier transform (FFT), as described in Section 2. The strain-hardening model will be implemented in the context of the linear self-consistent formulation, described in Section 3. The difficulties associated with the introduction of local hardening laws are explained in Section 4, and an improved procedure is proposed. In Section 5 an application to two-dimensional polycrystals is presented.

2. Full-field computations

2.1. FFT-based formulation

The FFT-based full-field formulation for viscoplastic polycrystals, to be used as a reference solution for comparison with the results of statistical approaches, is conceived for periodic unit cells, provides an exact solution of the governing equations (equilibrium and compatibility), and has better numerical performance than a FE calculation for the same purpose and resolution. It was originally developed [42–44] as a fast algorithm to compute the elastic and elastoplastic effective and local response of composites and later adapted [38,39,45,46] to deal with the viscoplastic deformation of two- and three-dimensional linear and power-law polycrystals.

Briefly, the viscoplastic FFT-based formulation consists in finding a strain rate field, associated with a kinematically admissible velocity field, which minimizes the average of

local work rate, under the compatibility and equilibrium constraints. The method is based on the fact that the local mechanical response of a periodic heterogeneous medium can be calculated as a convolution integral between the Green function of a linear reference homogeneous medium and the actual heterogeneity field. Since such types of integrals reduce to a simple product in Fourier space, the FFT algorithm can be used to transform the heterogeneity field into Fourier space and, in turn, get the mechanical fields by antitransforming that product back to real space. However, the actual heterogeneity field depends precisely on the a priori unknown mechanical fields. Therefore an iterative scheme should be implemented to obtain upon convergence a compatible strain-rate field and a stress field in equilibrium (see Refs. [38,44] for details).

It is worth noting that, since the FFT solution corresponds to a particular unit cell configuration, a thorough comparison with statistical results would require one to perform ensemble averages over a number of random configurations. However, it has been shown [38,39,46] that in the present case of linearly viscous polycrystals, with almost isotropic effective behavior and moderate anisotropy at local level, the dispersion of results for different configurations is rather small. Therefore, for the comparisons below, a single unit cell has been considered.

2.2. Local constitutive behavior

Let us consider a model polycrystal made of columnar orthorhombic grains with symmetry axes aligned with the macroscopic axis x_3 such that, when it is loaded in the anti-plane mode with shearing direction along x_3 , the only two slip systems that can be activated in the grains are those defined by the following Schmid tensors:

$$\mathbf{R}_1 = (\mathbf{e}_1 \otimes \mathbf{e}_3 + \mathbf{e}_3 \otimes \mathbf{e}_1)/2, \quad \mathbf{R}_2 = (\mathbf{e}_2 \otimes \mathbf{e}_3 + \mathbf{e}_3 \otimes \mathbf{e}_2)/2 \quad (1)$$

where $\{\mathbf{e}_1, \mathbf{e}_2, \mathbf{e}_3\}$ is an orthonormal basis of crystallographic axes such that \mathbf{e}_3 is the slip direction of both systems, and \mathbf{e}_1 and \mathbf{e}_2 are the slip plane normal of systems 1 and 2, respectively. By further considering that the material is incompressible and that \mathbf{e}_3 lies parallel to x_3 , the problem becomes two-dimensional. Macroscopic and local stresses ($\bar{\boldsymbol{\sigma}}$ and $\boldsymbol{\sigma}(\mathbf{x})$, respectively) and strain rates ($\bar{\dot{\boldsymbol{\epsilon}}}$ and $\dot{\boldsymbol{\epsilon}}(\mathbf{x})$, respectively) are thus characterized by two-dimensional vectors formed by the 13 and 23 components of the corresponding tensors. The local viscous stiffness tensor $\mathbf{L} = 2\bar{\boldsymbol{\mu}}$ can be reduced to a two-dimensional symmetric second-order tensor with diagonal components $2\mu_{11} = 2\mu_{1313}$, $2\mu_{22} = 2\mu_{2323}$ and off-diagonal components $2\mu_{12} = 2\mu_{1323}$. The linear constitutive relation reads

$$\dot{\boldsymbol{\epsilon}}(\mathbf{x}) = \mathbf{L}^{-1}(\mathbf{x}) : \boldsymbol{\sigma}(\mathbf{x}) = \dot{\gamma}_0 \sum_{k=1}^2 \frac{\mathbf{R}_k(\mathbf{x}) \otimes \mathbf{R}_k(\mathbf{x})}{\tau_{0k}(\mathbf{x})} : \boldsymbol{\sigma}(\mathbf{x}) \quad (2)$$

where τ_{01} and τ_{02} are the RRSS of systems 1 and 2, and $\dot{\gamma}_0$ is a reference slip rate.

In this work we do not consider the effect of geometrical hardening (lattice rotation during the plastic deformation). Rather, we concentrate on the effects of work hardening (interaction between dislocations) only. Therefore, the lattice orientation within each grain is assumed to remain constant throughout the deformation process. Evidently, such an assumption does not represent the behavior of real materials, but it is justified in the context of this model study since the available treatment of lattice rotations under the SC scheme suffers from the same limitations as the work hardening: it does not depend on the intraphase strain heterogeneity. Therefore, in order to remove any bias from the comparison between the SC and the FFT results, lattice orientation is disregarded in both models. Furthermore, the crystallographic orientation is assumed uniform within each grain (i.e. no intragranular misorientation), so that Schmid tensors also become uniform. Consequently, Eq. (2) now reads

$$\dot{\boldsymbol{\epsilon}}(\mathbf{x}) = \dot{\gamma}_0 \sum_r \chi^{(r)}(\mathbf{x}) \sum_{k=1}^2 \frac{\mathbf{R}_k^r \otimes \mathbf{R}_k^r}{\tau_{0k}(\mathbf{x})} : \boldsymbol{\sigma}(\mathbf{x}) \quad (3)$$

where the characteristic function $\chi^{(r)}(\mathbf{x})$, which is equal to 1 if the position vector \mathbf{x} is inside a grain with the crystalline orientation (r) and zero otherwise, has been introduced.

Hereafter, we assume that at the initial deformation stage the RRSS of each slip system is uniform throughout the polycrystal, with the convention $\tau_{01} < \tau_{02}$ (system 1 is “softer” than system 2). Hence, the initial viscous compliance is also uniform within each grain. Under these conditions it can be shown [47,48] that, if the polycrystal is macroscopically isotropic, the overall viscous stiffness $\bar{\mathbf{L}} = 2\bar{\boldsymbol{\mu}}$ (such that $\bar{\dot{\boldsymbol{\epsilon}}} = \bar{\mathbf{L}}^{-1} : \bar{\boldsymbol{\sigma}}$ is diagonal, i.e. $\bar{\mu}_{11} = \bar{\mu}_{22} (= \bar{\mu})$ and $\bar{\mu}_{12} = 0$, and obeys

$$\det(\bar{\boldsymbol{\mu}}) = \bar{\mu}^2 = \tau_{01} \tau_{02} \quad (4)$$

However, it is emphasized that, as soon as the RRSS of each slip system is no more uniform within the grains, the simple analytical relation (Eq. (4)) does not hold any more.

At the slip system level, the constitutive relation reads

$$\dot{\gamma}_k(\mathbf{x}) = \dot{\gamma}_0 \frac{\tau_k(\mathbf{x})}{\tau_{0k}(\mathbf{x})} \quad (5)$$

The resolved shear stress on slip system k is given by

$$\tau_k(\mathbf{x}) = \mathbf{R}_k(\mathbf{x}) : \boldsymbol{\sigma}(\mathbf{x}) = \sum_{r=1}^N \chi^{(r)}(\mathbf{x}) \mathbf{R}_k^r(\mathbf{x}) : \boldsymbol{\sigma}(\mathbf{x}) \quad (6)$$

In addition, if strain hardening is considered adopting the theoretical framework of Mandel [2] and Hill [3], the time derivative of the RRSS on slip system (k), $\dot{\tau}_{0k}$, and the shear rates $\dot{\gamma}_{k'}$ on each slip system are linked according to

$$\dot{\tau}_{0k}(\mathbf{x}) = \sum_{k'} h_{kk'}(\mathbf{x}) |\dot{\gamma}_{k'}(\mathbf{x})| \quad (7)$$

with h being the instantaneous hardening matrix. Its diagonal (h_{kk}) and off-diagonal ($h_{kk'}$, $k \neq k'$) components

express, respectively, the self- and latent hardening. In general, Eq. (7) is a nonlinear relation, since h depends on the accumulated strain.

2.3. Microstructure

The microstructure considered in this work is a periodic square two-dimensional unit cell generated by Voronoi tessellation. Such a microstructure has been chosen for the sake of its simplicity. The resulting two-dimensional polycrystal is made of 8500 grains. The crystallographic orientation of each grain is defined by an angle, denoted θ , between the crystallographic axis \mathbf{e}_1 of the grain and the macroscopic axis x_1 . In what follows, a mechanical phase will be defined by the set of grains exhibiting the same θ value, i.e. the same initial mechanical behavior. In order to guarantee that (i) the orientation of each grain differs from those of its direct neighbors, (ii) the volume fractions of each mechanical phase are equal and (iii) the microstructure exhibits, at the first loading stage, an isotropic overall behavior, eight different values of θ were chosen ($\theta = 0^\circ, 22.5^\circ, 45^\circ, 67.5^\circ, 90^\circ, 112.5^\circ, 135^\circ$ and 157.5°). It is then possible to identify the softest ($\theta = 0^\circ$) and the hardest ($\theta = 90^\circ$) phase (called in what follows “soft” and “hard” phase, respectively), a classification that will be useful when discussing the local shear rate distributions. For the FFT computations, a regular Fourier grid of 512×512 points

has been used to discretize the unit cell, leading to an average of about 30.8 Fourier points within each grain and 32,768 points within each mechanical phase (for more details concerning the construction and characterization of this two-dimensional Voronoi microstructure, see Ref. [46]).

2.4. FFT results

The local behavior of our model two-dimensional polycrystal is characterized by an initial contrast τ_{02}/τ_{01} and a linear hardening (constant matrix h) with $h_{kk}/\tau_{01} = 1$ and $h_{kk'} = 1.5h_{kk}$. The choice of such a high contrast value between the soft and the hard slip systems is necessary, in the present context of linear viscosity, to have one system significantly more active than the other. The computations of mechanical behavior were performed for a macroscopic strain rate $\dot{\bar{\epsilon}} = 10^{-2} \text{ s}^{-1}$ applied in incremental deformation steps of 0.01, up to an overall strain of 0.2.

The probability densities corresponding to the values of the slip rate field $\dot{\gamma}(\mathbf{x})$ evaluated in the Fourier points, for the two slip systems of the “soft” mechanical phase (at 0°) are given in Fig. 1, for the initial ($\bar{\epsilon}_{13} = 0$) and final ($\bar{\epsilon}_{13} = 0.2$) deformation steps. Simple geometrical considerations show that slip system 1 in this phase is expected to be the most active system of the whole polycrystal. The corresponding slip rates are thus relatively high and positive

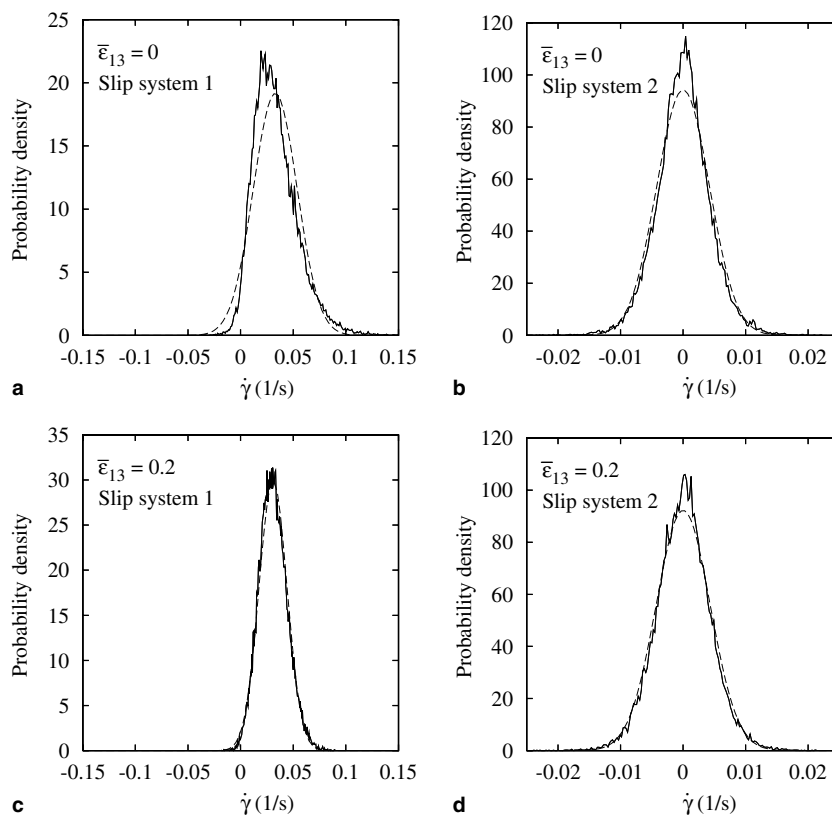


Fig. 1. Slip rate distributions obtained with the FFT method (solid lines) in the “soft” phase ($\theta = 0^\circ$) for both slip systems, at macroscopic strains $\bar{\epsilon}_{13} = 0$ (a, b) and $\bar{\epsilon}_{13} = 0.2$ (c, d). The dashed lines indicate the corresponding Gaussian approximations.

almost everywhere, both at the initial and final deformation steps. Nevertheless, the slip rate on this “best-oriented” slip system becomes null or even negative at some particular locations. In other words, the most active system in the whole polycrystal can, at certain locations, slip in the “reverse” direction. This observation highlights the effects of the highly heterogeneous stress distribution in the polycrystal, which originates from the interaction between neighboring grains. Similar conclusions can be drawn for system 2 of the same phase. This system is the “worst-oriented” system of the whole polycrystal with the highest RRSS, and, on average, does not glide since the mean value of the resolved shear stress vanishes. However, its distribution exhibits a non-negligible width, indicating that significant positive or negative slip appear locally, due to intergranular interactions. Consequently, this system should contribute significantly to the work hardening of the polycrystal (see Eq. (7)). Similar observations, not reported here for conciseness, have been made analyzing the distributions of slip activity in the other phases.

It is interesting at this point to approximate the observed shear rate distributions by classic probability functions. To this end, we have computed the first and second moments of the probability densities obtained by means of the FFT computations, and used these two quantities to determine the position and the width of the analytical probability functions that approximate the actual

distributions. Given that we are not accounting for higher order statistical moments (the reason for which is explained in the sequel), we are limited to probability functions that depend on only two parameters. The resulting Gaussian distributions have been superimposed to the probability densities of Fig. 1. It can be observed that the slip rate distribution of the most active system (system 1) is not strictly Gaussian initially, showing a marked asymmetry with a slowly decreasing tail at large slip rates. However, as deformation proceeds, it becomes more symmetric and narrower. For the harder system (system 2) the probability densities appear to be almost symmetric throughout the deformation process. Similar distributions have been obtained for the other phases meaning that the Gaussian distribution appears to be an appropriate analytical function to approximate the actual shear rate distributions. A similar conclusion has been drawn in Ref. [49] in the case of two-dimensional two-phase composites made of isotropic linear phases, having “particulate” (i.e. matrix-inclusion) microstructures. Hence, the Gaussian distribution is likely to be well adapted to linearly viscous heterogeneous materials, independently of their microstructures.

Due to the heterogeneity of the slip rates, the initially uniform reference stresses τ_{0k} in the phases become non-uniform as deformation proceeds (see Eq. (7)). This is illustrated by the distributions of τ_{0k} after 0.2 macroscopic shear strain (Fig. 2). These distributions are evidently

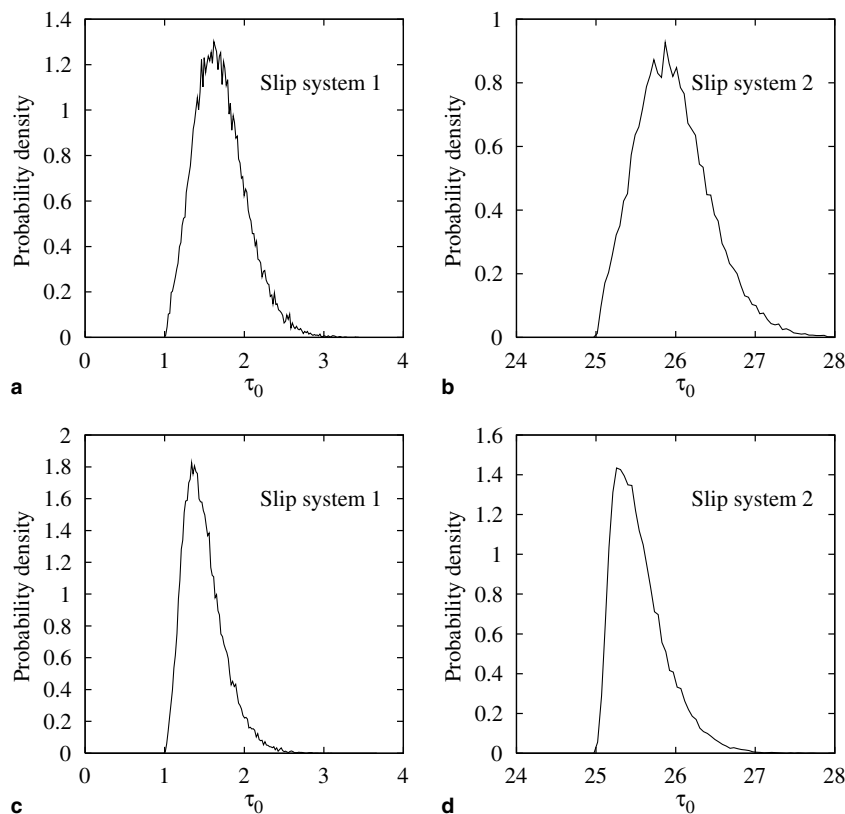


Fig. 2. RRSS distributions (in units of the initial τ_0) in the “soft” phase ($\theta = 0^\circ$) (a, b) and the “hard” phase ($\theta = 90^\circ$) (c, d), for $\bar{\epsilon}_{13} = 0.2$. The probability densities for $\bar{\epsilon}_{13} = 0$ are Dirac’s deltas at $\tau_0 = 1$ and $\tau_0 = 25$, respectively.

non-symmetric, with a long and slowly decreasing tail at large τ_0 values. In the “soft” phase ($\theta = 0^\circ$) slip system 1 is by far the most active system and therefore hardens mainly due to self-hardening, while slip system 2 is less active and hardens mainly by latent hardening. The distribution width for system 2 is larger than that for slip system 1, by a factor of about 1.5, in agreement with the ratio between off-diagonal and diagonal elements of the hardening matrix h . For the “hard” phase ($\theta = 90^\circ$), none of the slip systems glides significantly so that this phase hardens less than the one at $\theta = 0^\circ$. Consequently, the τ_0 distributions are narrower.

In light of the above results, the next section shows how to formulate meaningful work-hardening laws using intra-phase statistical information, when more efficient mean-field formulations — instead of numerically demanding full-field approaches — are used to describe the mechanical evolution of viscoplastic polycrystals.

3. Mean-field estimates

A polycrystal can be considered as a composite material made of N crystalline orientations. Each orientation (r) defines a mechanical phase whose spatial repartition is entirely described by the characteristic function $\chi^{(r)}(\mathbf{x})$ previously introduced. However, considering the random character of a polycrystalline microstructure, it is not worth trying to determine every detail of $\chi^{(r)}(\mathbf{x})$. Instead, the microstructure can be described statistically by the correlation functions of the characteristic functions. For instance, the knowledge of the volume fractions $c_r = \langle \chi^{(r)}(\mathbf{x}) \rangle$ (where $\langle \dots \rangle$ denotes the volume average over the representative volume element (RVE)) allows the derivation of the classic Reuss and Voigt bounds for the overall behavior. Furthermore, additional assumptions on the covariances $\varphi_{rs} = \langle \chi^{(r)}(\mathbf{x}) \chi^{(s)}(\mathbf{x} + \mathbf{h}) \rangle$ (where \mathbf{h} is a position vector) can be used to derive the sharper Hashin–Shtrikman bounds. Moreover, due to the “granular” character of a polycrystal (i.e. all phases are on the same footing), the SC estimates [50] are well adapted for these kinds of microstructures. According to Kröner [51], the SC scheme provides the exact solution for so-called perfectly disordered random microstructures, characterized by the fact that all — i.e. up to infinite order — correlation functions are statistically homogeneous, isotropic, and disordered.

Let us consider the class of constitutive behavior which reads

$$\dot{\boldsymbol{\epsilon}}(\mathbf{x}) = \mathbf{M}(\mathbf{x}) : \boldsymbol{\sigma}(\mathbf{x}) \quad (8)$$

where (see Eq. (2))

$$\mathbf{M}(\mathbf{x}) = \mathbf{L}^{-1}(\mathbf{x}) = \dot{\gamma}_0 \sum_{k=1}^2 \frac{\mathbf{R}_k(\mathbf{x}) \otimes \mathbf{R}_k(\mathbf{x})}{\tau_{0k}(\mathbf{x})} \quad (9)$$

is the local viscous compliance tensor. Let us further assume that the RVE is subjected to a uniform stress field

$\bar{\boldsymbol{\sigma}}$. Because of the limited information available on the microstructure, the localization problem linking the local stress field $\boldsymbol{\sigma}(\mathbf{x})$ to the macroscopic loading cannot be solved. Nevertheless, using the statistical description of the microstructure, the problem can be degenerated, considering only the average localization for each mechanical phase.

In this context, the linear SC scheme has been proposed for dealing with materials for which the mechanical properties are uniform within each mechanical phase, so that

$$\mathbf{M}(\mathbf{x}) = \sum_{r=1}^N \mathbf{M}^{(r)} \chi^{(r)}(\mathbf{x}) \quad (10)$$

with $\mathbf{M}^{(r)}$ the compliance of phase (r). In the present case, given that the RRSSs are assumed initially uniform, the above condition is strictly valid at the first deformation increment. However, as deformation proceeds, the slip rate heterogeneities induce a non-uniformity of $\tau_{0k}^{(r)}$ and thus of $\mathbf{M}(\mathbf{x})$. Therefore, since Eq. (10) is used explicitly in the derivation of the SC equations, some sort of approximation is necessary to apply this formulation in subsequent deformation increments. The consequences of such an approximation are discussed in the next section.

Using an additional assumption of ellipsoidal shape for the covariances φ_{rs} [52], the estimation of the overall compliance tensor $\widetilde{\mathbf{M}}$ can be made using Eshelby’s solution [53] for an ellipsoidal inclusion embedded in an infinite homogeneous linear medium, itself subjected to a homogeneous loading. The SC expression of $\widetilde{\mathbf{M}}$ is given by solution of the following equation:

$$\widetilde{\mathbf{M}} = \langle (\mathbf{M}^* + \mathbf{M}^{(r)})^{-1} \rangle^{-1} - \mathbf{M}^* \quad (11)$$

where \mathbf{M}^* is the inverse of the “constraint” tensor introduced by Hill [54] which reflects the reaction of the homogeneous medium to the deformation rate of the inclusion, and is given by

$$\mathbf{M}^* = (\mathbf{P}^{-1} - \widetilde{\mathbf{M}}^{-1})^{-1} \quad (12)$$

which makes Eq. (11) implicit. \mathbf{P} is a microstructural tensor that depends on the overall compliance and on the shape of the inclusion.

The phase average localization tensor can be then obtained as

$$\langle \mathbf{B} \rangle_r = (\mathbf{M}^{(r)} + \mathbf{M}^*)^{-1} : (\widetilde{\mathbf{M}} + \mathbf{M}^*) \quad (13)$$

where $\langle \dots \rangle_r$ indicates the volume average over the volume of phase (r). The phase average stress tensor is given by

$$\langle \boldsymbol{\sigma} \rangle_r = \langle \mathbf{B} \rangle_r : \bar{\boldsymbol{\sigma}} \quad (14)$$

The knowledge of $\langle \boldsymbol{\sigma} \rangle_r$, i.e. the first-order moment of the stress distribution in phase (r), provides an initial insight into the local stress statistics. Additional information can be obtained in terms of the second-order moment of the stress in the phase $\langle \boldsymbol{\sigma} \otimes \boldsymbol{\sigma} \rangle_r$, which can be calculated by derivation of the effective potential with respect to the local compliance [35]:

$$\langle \boldsymbol{\sigma} \otimes \boldsymbol{\sigma} \rangle_r = \frac{1}{c_r} (\bar{\boldsymbol{\sigma}} \otimes \bar{\boldsymbol{\sigma}}) :: \frac{\partial \widetilde{\mathbf{M}}}{\partial \mathbf{M}^{(r)}} \quad (15)$$

Expressions analogous to Eqs. (14) and (15) hold for the strain rate moments within each phase. Alternatively, the statistical moments of $\dot{\boldsymbol{\varepsilon}}$ can be obtained from the constitutive relation Eq. (8):

$$\langle \dot{\boldsymbol{\varepsilon}} \rangle_r = \mathbf{M}^{(r)} : \langle \boldsymbol{\sigma} \rangle_r, \quad \langle \dot{\boldsymbol{\varepsilon}} \otimes \dot{\boldsymbol{\varepsilon}} \rangle = \mathbf{M}^{(r)} : \langle \boldsymbol{\sigma} \otimes \boldsymbol{\sigma} \rangle_r : \mathbf{M}^{(r)} \quad (16)$$

It has been shown in Ref. [36] that, in the context of a general anisotropy and for an arbitrary number of phases, the partial derivatives appearing in Eq. (15) can be obtained as solutions of simple linear systems. It is also worth mentioning that at present there are no expressions available for the estimation of statistical moments higher than order 2.

From Eq. (6), the first and second moments of the resolved shear stress on a slip system k read

$$\langle \tau_k \rangle_r = \mathbf{R}_k^{(r)} : \langle \boldsymbol{\sigma} \rangle_r, \quad \langle \tau_k^2 \rangle_r = \mathbf{R}_k^{(r)} : \langle \boldsymbol{\sigma} \otimes \boldsymbol{\sigma} \rangle_r : \mathbf{R}_k^{(r)} \quad (17)$$

from where the standard deviation ($\langle \tau_k^2 \rangle_r - \langle \tau_k \rangle_r^2$)^{1/2} can be computed. If RRSS fields are uniform within each phase and for each slip system, i.e.

$$\tau_{0k}(\mathbf{x}) = \sum_{r=1}^M \tau_{0k}^{(r)} \chi^{(r)}(\mathbf{x}) \quad (18)$$

the first and second moments of the shear rates can be computed rigorously:

$$\langle \dot{\gamma}_k \rangle_r = \frac{\dot{\gamma}_0}{\tau_{0k}^{(r)}} \langle \tau_k \rangle_r, \quad \langle \dot{\gamma}_k^2 \rangle_r = \left(\frac{\dot{\gamma}_0}{\tau_{0k}^{(r)}} \right)^2 \langle \tau_k^2 \rangle_r \quad (19)$$

If Eq. (18) holds, it has been proved — for the present RVE configuration and linearly viscous constitutive behavior — that the SC estimates of the first and second moments of mechanical fields are in general in very good agreement with those obtained by means of direct statistics performed on the full-field FFT solution [46]. Otherwise, if τ_{0k} are functions of the position inside each phase, the local compliance is not piecewise uniform, and the definition of $\mathbf{M}^{(r)}$ is not straightforward. In particular, the estimation of the

slip rate moments requires the evaluation of $\langle \tau_k / \tau_{0k} \rangle_r$ and $\langle \tau_k^2 / \tau_{0k}^2 \rangle_r$, which, in general, is not a trivial task.

4. Improved treatment for work hardening

4.1. Standard procedure

As already mentioned, in most applications of the SC scheme found in the literature, the intraphase heterogeneities of stress and strain rate are not considered. The typical assumption for the slip rate field is that $\dot{\gamma}_k(\mathbf{x})$ can be approximated by $\langle \dot{\gamma}_k \rangle_r$ (denoted $\dot{\gamma}_k^{(r)}$ in what follows) for all \mathbf{x} belonging to the phase (r). It follows that, if both the hardening matrix h and the RRSSs τ_{0k} are uniform within each phase and for each slip system before loading, then these quantities will remain uniform throughout the deformation process. Hence, in this case, the hardening law Eq. (7) reduces to

$$\dot{\tau}_{0k}^{(r)} = \sum_{k'} h_{kk'}^{(r)} |\dot{\gamma}_{k'}^{(r)}| \quad (20)$$

Consequently, a slip system that on average does not glide, i.e. for which $\dot{\gamma}_k^{(r)} = 0$, does not contribute to the overall hardening of the polycrystal.

This approximation is obviously too simple and therefore not accurate. Indeed, the full-field computations discussed in Section 2.4 clearly show that local slip takes place even if the average slip rate vanishes. An important consequence is that those “hard” slip systems also contribute to the global hardening of the material. By disregarding this physical evidence, the standard treatment leads to a global underestimation of the real hardening rate. This is illustrated in Fig. 3 where the SC predictions (using the standard hardening assumption) of the phase average RRSSs are compared with those obtained with tile FFT method. It can be seen that the standard treatment underestimates particularly the hardening of the two slip systems of the “hard” phase ($\theta = 90^\circ$). This is fully consistent with the above remarks, since for this phase the average slip rate vanishes for slip system 1, and it is also close to zero for slip

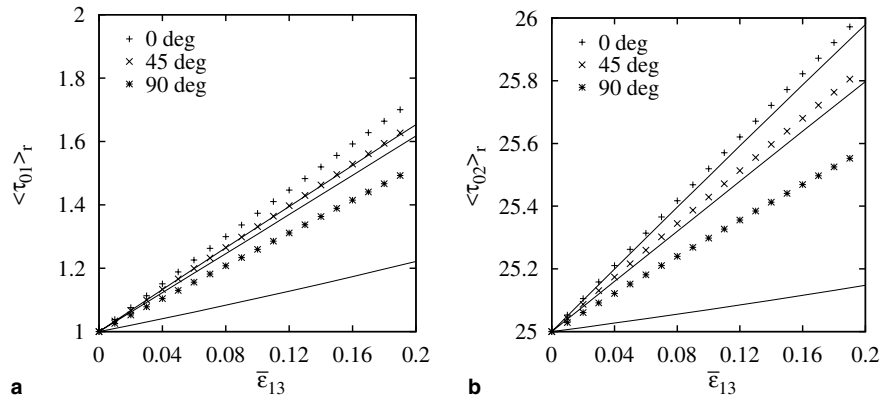


Fig. 3. Evolution of the phase average RRSSs during antiplane deformation on (a) slip system 1 and (b) slip system 2, within phases at $\theta = 0^\circ, 45^\circ$ and 90° . The FFT results (symbols) are compared with the standard procedure estimates (lines).

system 2, due to its high RRSS. Better results are obtained for the two other phases ($\theta = 0^\circ$ and $\theta = 45^\circ$). In both cases, the ratio between the hardening rate of the two slip systems of the phase is close to 1.5, showing that the slip rates on the soft system 1 are the ones that mostly contribute to the local hardening of both slip systems.

4.2. Using slip rate fluctuations

The above discussions lead to the conclusion that there are at least two major difficulties to overcome for an improved treatment of polycrystal work hardening using mean-field approaches. Firstly, one has to deal with RRSSs (and therefore local compliances) that are not uniform in the phases, as discussed in Section 3. Secondly, the intra-phase slip rate heterogeneity has to be accounted for, as discussed in Section 4.1. Furthermore, a third complication can arise from the fact that, unless a very simple form of the hardening matrix is adopted (like in the present case of constant h), this matrix can also become heterogeneous inside a mechanical phase as deformation proceeds. For the sake of simplicity, the latter situation will not be considered in the present work.

In order to address the first difficulty, it is necessary to define a phase uniform compliance $\mathbf{M}^{(r)}$ to allow the application of the classic homogenization scheme of Section 3. One possibility would be to divide each mechanical phase into many “sub-phases” in which τ_{0k} can be considered uniform, at least for a given deformation increment. In this way, the continuously varying field of compliances would be replaced by a piecewise constant approximation. The advantage of such a scheme is that its accuracy can be increased by increasing the number of sub-phases, but this procedure would increase exponentially the number of sub-phases as deformation proceeds, something inconvenient for practical applications. The second possibility consists in determining the compliance $\mathbf{M}^{(r)}$ that best describes the phase behavior “on average”, according to the available information on $\tau(\mathbf{x})$ and $\dot{\gamma}(\mathbf{x})$. This solution is explored in what follows.

The application of the SC scheme requires a local constitutive relation of the form

$$\langle \dot{\boldsymbol{\varepsilon}} \rangle_r = \mathbf{M}^{(r)} : \langle \boldsymbol{\sigma} \rangle_r = \dot{\gamma}_0 \sum_k \mathbf{R}_k^{(r)} \left\langle \frac{\tau_k}{\tau_{0k}} \right\rangle_r \quad (21)$$

As already mentioned, the exact evaluation of $\langle \tau_k / \tau_{0k} \rangle_r$, and thus of $\mathbf{M}^{(r)}$, is not possible. To overcome this difficulty, at least approximately, one may decompose the RRSS field into

$$\tau_{0k}(\mathbf{x}) = \langle \tau_{0k} \rangle_r + \delta\tau_{0k}(\mathbf{x}) \quad (22)$$

If one further assumes that the fluctuation term $\delta\tau_{0k}(\mathbf{x})$ is small compared with the mean value $\langle \tau_{0k} \rangle_r$ (according to Fig. 2, this approximation may be rather coarse for the soft slip system 1, but it is rather reasonable for the hard system 2), the first-order Taylor expansion of the above expression leads to

$$\left\langle \frac{\tau_k}{\tau_{0k}} \right\rangle_r \approx \frac{\langle \tau_k \rangle_r}{\langle \tau_{0k} \rangle_r} - \frac{\langle \tau_k \tau_{0k} \rangle_r - \langle \tau_k \rangle_r \langle \tau_{0k} \rangle_r}{\langle \tau_{0k} \rangle_r^2} \quad (23)$$

The second term on the right-hand side, which expresses the correlation between $\tau_k(\mathbf{x})$ and $\tau_{0k}(\mathbf{x})$, cannot be evaluated in the context of mean-field approaches. Taking this correlation into account would require a specific procedure to homogenize the behavior of each mechanical phase, i.e. to estimate its effective behavior with respect to the distribution of the mechanical heterogeneity within the phase. Consequently, the approximation is limited here to the zeroth-order term. Hence

$$\langle \dot{\gamma}_k \rangle_r = \dot{\gamma}_0 \langle \tau_k / \tau_{0k} \rangle_r \approx \dot{\gamma}_0 \langle \tau_k \rangle_r / \langle \tau_{0k} \rangle_r \quad (24)$$

Replacing the latter in Eq. (21), the approximate expression of $\mathbf{M}^{(r)}$ results:

$$\mathbf{M}^{(r)} \approx \dot{\gamma}_0 \sum_k \frac{\mathbf{R}_k^{(r)} \otimes \mathbf{R}_k^{(r)}}{\langle \tau_{0k} \rangle_r} \quad (25)$$

Hence, to obtain incremental estimations of $\mathbf{M}^{(r)}$, the evolution of $\langle \tau_{0k} \rangle_r$ with the deformation has to be evaluated averaging the hardening law in the phases, i.e.

$$\langle \dot{\tau}_{0k} \rangle_r = \sum_{k'} \langle h_{kk'} |\dot{\gamma}_{k'}| \rangle_r \quad (26)$$

Even in the simplest case, where $h_{kk'}$ is uniform within each phase, the computation of $\langle |\dot{\gamma}_k| \rangle_r$ is required. This, in general, is not possible, since only $\langle \dot{\gamma}_k \rangle_r$ and $\langle \dot{\gamma}_k^2 \rangle_r$ are known. Therefore, additional assumptions are necessary. Assuming that the $\dot{\gamma}_k$ distributions are Gaussian, one obtains

$$\langle |\dot{\gamma}_k| \rangle_r = \mu \operatorname{erf}(\beta) + \sqrt{\frac{2}{\pi}} \sigma \exp(-\beta^2) \quad (27)$$

where $\mu = \langle \dot{\gamma}_k \rangle_r$ is the mean value of the $\dot{\gamma}_k$ distribution in phase (r), $\sigma = \sqrt{\langle \dot{\gamma}_k^2 \rangle_r - \langle \dot{\gamma}_k \rangle_r^2}$ is the corresponding standard deviation, and $\beta = \mu / (\sqrt{2}\sigma)$. Note that this is the best approximation based on analytical functions that can be obtained since, as discussed earlier, homogenization techniques only provide two statistical parameters of the intra-phase distribution.

To assess the error introduced by the above approximation, we have compared the values of $\langle |\dot{\gamma}_k| \rangle_r$ as functions of $\langle \dot{\gamma}_k \rangle_r$, computed directly from the full-field results, and obtained by approximating the $\dot{\gamma}_k$ distributions by Gaussians with the same average and standard deviation as the actual full-field distribution (Fig. 4). Clearly, the Gaussian approximation provides a good representation of the actual distributions. The matching is almost exact at $\varepsilon_{13} = 0.2$ since, as already shown in Fig. 1, the $\dot{\gamma}_k$ distributions tend to be more symmetric as deformation increases.

Another interesting observation from Fig. 4 is that the approximation $\langle |\dot{\gamma}_k| \rangle_r \approx |\langle \dot{\gamma}_k \rangle_r|$, illustrated by the dashed line and implicitly assumed in the standard procedure, does not deliver accurate results, especially for the harder systems.

Finally, it should be remarked that, while the second moment of the $\dot{\gamma}_k$ distribution in phase (r), given by

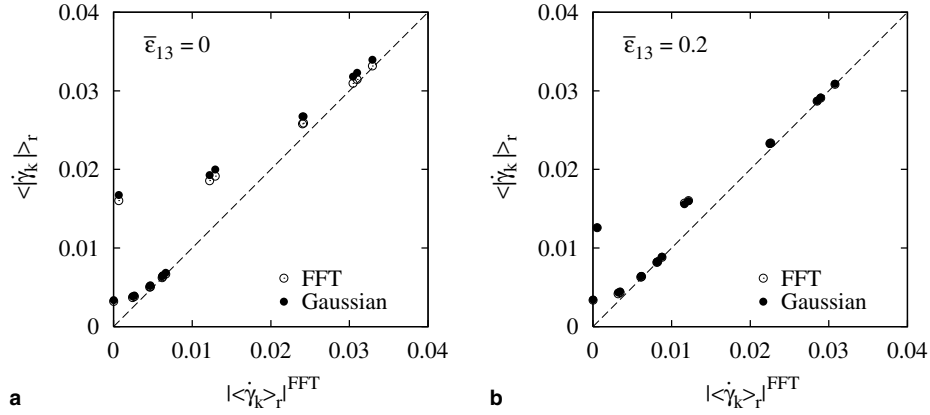


Fig. 4. $\langle |\dot{\gamma}_k| \rangle_r$ as functions of $|\langle \dot{\gamma}_k \rangle_r|^{\text{FFT}}$ for both slip systems in every phase, obtained directly from FFT results (open circles) and approximating the actual $\dot{\gamma}_k$ distributions by Gaussians (filled circles), for (a) the initial and (b) the final deformation increments. In (b), the two sets of points are completely overlapped.

$$\langle \dot{\gamma}_k^2 \rangle_r = \dot{\gamma}_0^2 \left\langle \frac{\tau_k^2}{\tau_{0k}^2} \right\rangle_r \quad (28)$$

is also needed to evaluate $\langle |\dot{\gamma}_k| \rangle_r$ (Eq. (27)), it cannot be calculated by mean-field approaches. Instead, replacing Eq. (23) in Eq. (28), the following approximate expression is obtained:

$$\langle \dot{\gamma}_k^2 \rangle_r \approx \dot{\gamma}_0^2 \left[\frac{\langle \tau_k^2 \rangle_r}{\langle \tau_{0k} \rangle_r^2} - 2 \frac{\langle \tau_k^2 \tau_{0k} \rangle_r - \langle \tau_k^2 \rangle_r \langle \tau_{0k} \rangle_r}{\langle \tau_{0k} \rangle_r^3} \right] \quad (29)$$

However, as explained earlier, only the first term of the above development can be retained, i.e.

$$\langle \dot{\gamma}_k^2 \rangle_r \approx \dot{\gamma}_0^2 \left[\frac{\langle \tau_k^2 \rangle_r}{\langle \tau_{0k} \rangle_r^2} \right] \quad (30)$$

5. Application to the two-dimensional polycrystal

The improved mean-field hardening treatment described above (to be referred to in what follows as the Gaussian SC approach) has been applied to the antiplane deformation of the two-dimensional polycrystal under consideration. The

evolution with deformation of the RRSSs of each slip system in phases at 0° , 45° and 90° is shown in Fig. 5. Compared with the results of the standard procedure (Fig. 3), the proposed hardening scheme represents a significant improvement. Using the Gaussian assumption for the slip rate distribution, the RSS evolution appears to be very close to the full-field reference solution for all phases and all slip systems. Note that the largest improvement was obtained for the hard slip systems, i.e. those belonging to the hard phase, since, for them, the standard procedure approximation $\langle |\dot{\gamma}_k| \rangle_r \approx |\langle \dot{\gamma}_k \rangle_r|$ has been proved to be rather inaccurate. This overall improvement at phase level is particularly important when mean-field approaches are intended to be used for the study of deformation-induced microstructure evolution, such as recrystallization. In such cases the activation mechanisms of these processes are strongly dependent on the energy stored in the grains during deformation, which in turn is closely related to the RRSS distributions. The proposed procedure is thus better adapted for quantitative estimations.

The predicted effective behavior of the two-dimensional polycrystal is shown in Fig. 6. The new procedure leads to

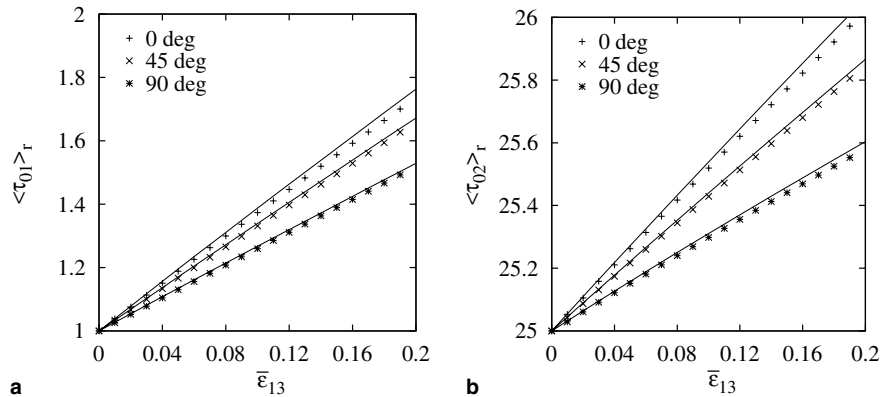


Fig. 5. Evolution of the phase average RRSSs during antiplane deformation on (a) slip system 1 and (b) slip system 2, within phases at $\theta = 0^\circ$, 45° and 90° . The FFT results (symbols) are compared with the “Gaussian” SC estimates (lines).

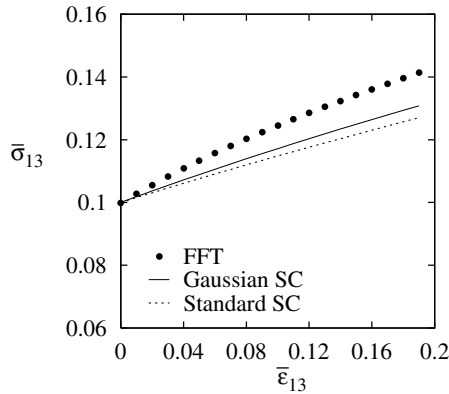


Fig. 6. Overall stress–strain response for antiplane shear mode. The reference full-field solution (symbols) is compared with the Gaussian SC (solid line) and the standard procedure (dashed line) estimates.

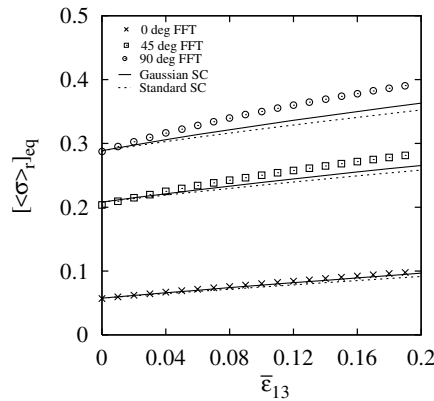


Fig. 7. Evolution with antiplane deformation of the average equivalent stress in the phases, for phases at $\theta = 0^\circ$, 45° and 90° . The full-field predictions (symbols) are compared with the Gaussian (solid lines) and standard (dotted lines) SC procedures.

a result that lies closer to the FFT reference solution than the standard hardening treatment. Nevertheless, although a clear improvement can be observed, a discrepancy still remains. Interestingly, whereas the average $\langle \tau_{0k} \rangle_r$ values

are slightly overestimated by the “Gaussian” SC estimate with respect to the FFT calculation (Fig. 5), the resulting overall behavior is markedly softer than the one predicted by the full-field computation. This result can only be attributed to the contribution to the overall hardening of the intraphase fluctuations of the τ_{0k} fields, which cannot be captured by the SC scheme, given the approximations that were necessary for the implementation described in Section 4.2.

Fig. 7 shows the evolution of the average equivalent stresses in the phases. Also at phase level the results obtained with the proposed hardening model are closer to the FFT solution than those of the standard procedure. The Gaussian SC estimation is very good for the soft phase. For the harder phases, the stress is globally underestimated, and the difference with the full-field values increases with strain. It can therefore be concluded that the differences between the mean-field and the full-field estimates of the macroscopic stress depicted in Fig. 6 are mainly due to the contribution of the harder mechanical phases.

At the level of each slip system, the first and second moments of $\dot{\gamma}_k$ obtained by means of the improved SC formulation (Eqs. (24) and (30)) can be compared with corresponding FFT reference values in terms of the following error quantities:

$$\Delta \dot{\gamma}_{kr} = \frac{\langle \dot{\gamma}_k \rangle_r^{\text{SC}} - \langle \dot{\gamma}_k \rangle_r^{\text{FFT}}}{\langle \dot{\gamma}_k \rangle_r^{\text{FFT}}} \quad \text{and} \quad \Delta \dot{\gamma}_{kr}^2 = \frac{\langle \dot{\gamma}_k^2 \rangle_r^{\text{SC}} - \langle \dot{\gamma}_k^2 \rangle_r^{\text{FFT}}}{\langle \dot{\gamma}_k^2 \rangle_r^{\text{FFT}}} \quad (31)$$

Very small values of $\Delta \dot{\gamma}_{kr}$ and $\Delta \dot{\gamma}_{kr}^2$ (of the order of 10^{-3}) — reflecting a very good agreement between the SC and the FFT predictions — have been reported and extensively discussed in Ref. [46] for the case in which τ_{0k} are uniform in the phases. In the present work the comparison is carried out at $\epsilon_{13} = 0.2$ (Fig. 8). A rather good agreement is also found in this case, given that the deviation is generally smaller than 10%. This shows that the SC formulation, when coupled with the proposed hardening procedure,

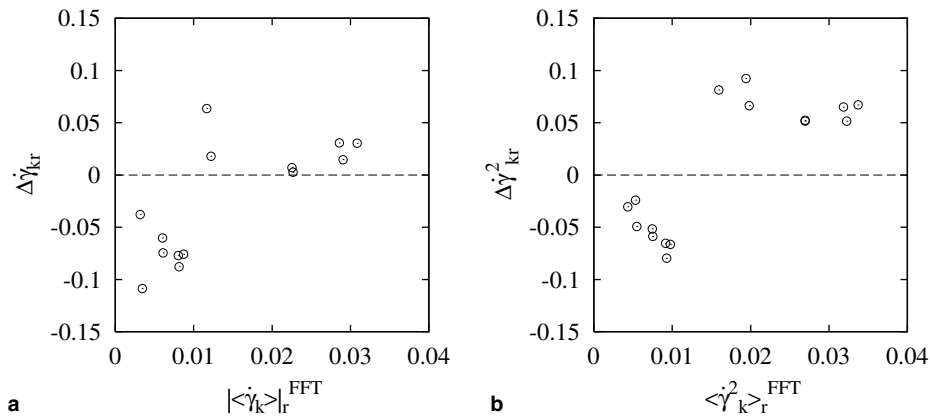


Fig. 8. Relative discrepancy between the SC predictions and the FFT solution for the intraphase (a) first and (b) second moments of the slip rate distributions for each slip system of each phase, for an accumulated deformation $\epsilon_{13} = 0.2$.

captures relatively well the heterogeneities in the material. However, it can be observed that the absolute values of the average slip rate $|\langle \dot{\gamma} \rangle_r^{\text{SC}}|$ for the hard slip systems are systematically smaller than the ones predicted with FFT, whereas the opposite is true for the soft slip systems. Similar conclusions are obtained for the second moments. It is also worth noting that the error on the phase average $\Delta \dot{\gamma}_{kr}$ is in general larger for the hard systems. One can thus conclude that, globally, better results are obtained with the present mean-field approach for the soft mechanical phases and the soft slip systems.

6. Concluding remarks

Some customary approximations made for the description and the numerical implementation of the work hardening of polycrystals by means of the SC model have been revisited. By comparing the results of the SC scheme for a two-dimensional linearly viscous polycrystal to those obtained with a full-field computation, it has been shown that the standard treatment of strain hardening neglects the effect of the intraphase strain heterogeneity. Since a slip system that does not glide on average does glide locally, its contribution to the global hardening of the material has to be considered. The procedure proposed in this work, addressing the proper averaging of the local hardening law, clearly improves the estimation of the global and the local material response. The mean values of RRSSs in the phases match very well with the full-field predictions. This improved feature of the SC model has important consequences for the study of deformation-induced microstructural evolutions, like recrystallization, which is driven by the stored energy and thus is directly linked to the RRSS distributions. From this point of view, the new approach should allow the use of the SC scheme to obtain real quantitative data.

Despite all the above encouraging results, the overall behavior estimated with the SC approach still departs from the reference solution. It is believed that this effect is related to the intraphase heterogeneity of the RRSS fields, which cannot be accounted for in the context of mean-field approaches. It has also been observed that more accurate results are obtained for the soft mechanical phases and the soft slip systems.

We have used the most simple hardening law in order to obtain simple results. However, in practice more realistic nonlinear laws, e.g. with h evolving with strain, should be considered. The proposed procedure can be extended to these cases. But additional difficulties can arise, since the intraphase fluctuation of h has to be considered in the summation appearing in Eq. (26). This term can probably be approximated by $\langle h_{kk'} \rangle_r \langle |\dot{\gamma}_{k'}| \rangle_r$, as long as the fluctuations of $h_{kk'}$ are not too large within the considered phase.

The present work is limited to polycrystals exhibiting a linear viscosity. Our investigation indicates that the extension to nonlinear viscoplasticity is not straightforward. Indeed, nonlinear FFT calculations have shown (e.g. Ref.

[49]) that the $\dot{\gamma}_k$ distributions are far from a Gaussian, with a marked asymmetry and a very long and slowly decreasing tail at large $\dot{\gamma}_k$ values. The use of the proposed procedure would require one to choose an adequate, non-symmetric distribution function. In this connection, at present, by using homogenization approaches it is only possible to calculate first and second moments of the mechanical fields. Therefore, only two-parameter distribution functions can be considered. Better results could be obtained if higher order statistical moments could be evaluated.

References

- [1] Taylor GI, Elam CF. Proc R Soc Lond 1923;A102:643–67.
- [2] Mandel J. Int J Solids Struct 1965;1:273–95.
- [3] Hill R. J Mech Phys Solids 1960;14:95–102.
- [4] Taylor GI. J Inst Metals 1938;62:307–24.
- [5] Kocks UF, Brown TJ. Acta Metall 1966;14:87–98.
- [6] Nakada Y, Keh AS. Acta Metall 1966;14:961–73.
- [7] Kocks UF. Metall Trans 1970;1:1121–43.
- [8] Franciosi P, Berveiller M, Zaoui A. Acta Metall 1980;28:773–83.
- [9] Kocks UF. J Eng Mater Technol 1976;10:76–85.
- [10] Chang YW, Asaro RJ. Acta Metall 1981;29:241–57.
- [11] Weng GJ. Int J Plast 1987;3:315–39.
- [12] Mecking H, Kocks UF. Acta Metall 1981;29:1865–75.
- [13] Teodosiu C, Raphanel JL, Tabourot L. In: Teodosiu C, Raphanel JL, Sidoroff F, editors. Large plastic deformations. Rotterdam; 1993. pp. 153–168.
- [14] Argon AS, Haasen P. Acta Metall Mater 1993;41:3289–306.
- [15] Peeters B, Seefeldt M, Teodosiu C, Kalidindi SR, van Houtte P, Aernoudt E. Acta Mater 2001;49:1607–19.
- [16] Estrin Y, Tóth LS, Molinari A, Bréchet Y. Acta Mater 1998;46:5509–22.
- [17] Langlois L, Berveiller M. Int J Plast 2003;19:599–624.
- [18] Peirce D, Asaro RJ, Needleman A. Acta Metall 1982;30:1087–119.
- [19] Tabourot L, Fivel M, Rauch E. Mater Sci Eng 1997;A234–236: 639–42.
- [20] Delaire F, Raphanel JL, Rey C. Acta Mater 2000;48:1075–87.
- [21] Hoc T, Crépin J, Gélébart L, Zaoui A. Acta Mater 2003;51:5477–88.
- [22] Bronkhorst CA, Kalidindi SR, Anand L. Proc R Soc Lond 1992;A341:443–77.
- [23] Becker R, Panchanadeeswaran S. Acta Metall Mater 1995;43: 2701–19.
- [24] Miller M, Dawson P. J Mech Phys Solids 1997;15:1781–804.
- [25] Zhou Y, Neale K, Tóth L. Int J Plast 1993;9:961–78.
- [26] Lin G, Havner KS. Int J Plast 1996;12:695–718.
- [27] Hutchinson JW. Proc R Soc Lond 1970;A319:247–72.
- [28] Berveiller M, Zaoui A. J Mech Phys Solids 1970;26:325–44.
- [29] Tóth LS, Molinari A. Acta Metall Mater 1994;42:2459–66.
- [30] Mercier S, Tóth L, Molinari A. Textures Microstruct 1995;25:45–61.
- [31] Pochettino AA, Sanchez P. In: Szpunar JA, editor. Proc. 12th Int. Conf. Textures of Materials. Canada: NRC Research Press; 1999.
- [32] Castelnau O, Francillette H, Bacroix B, Lebensohn RA. J Nucl Mater 2001;297:14–26.
- [33] Auslender F, Bornert M, Hoc T, Masson R, Zaoui A. In: Miehe C, editor. IUTAM Symposium on Computational Mechanics of Solid Materials at Large Strain, Canada, 2001.
- [34] Brenner R, Béchade J-L, Castelnau O, Bacroix B. J Nucl Mater 2002;305:175–86.
- [35] Ponte Castañeda P, Suquet P. Adv Appl Mech 1998;34:171–302.
- [36] Brenner R, Castelnau O, Badea L. Proc R Soc Lond 2004;A460:3589–612.
- [37] Lebensohn RA, Dawson PR, Kern HM, Wenk H-R. Tectonophysics 2003;370:287–311.

- [38] Lebensohn RA, Liu Y, Ponte Castañeda P. *Proc R Soc Lond* 2004;A460:1381–405.
- [39] Lebensohn RA, Liu Y, Ponte Castañeda P. *Acta Mater* 2004;52:5347–61.
- [40] Tomé CN, Lebensohn RA, Kaschner GC, Maudlin PJ. *Acta Mater* 2001;49:3085–96.
- [41] Commentz B, Hartig C, Mecking H. *Comput Mater Sci* 1999;16:237–47.
- [42] Moulinec H, Suquet P. *C R Acad Sci Paris* 1994;318:0417–1413.
- [43] Moulinec H, Suquet P. *Comput Meth Appl Mech Eng* 1998;157:69–94.
- [44] Michel J-C, Moulinec H, Suquet P. *Comput Model Eng Sci* 2000;1:79–88.
- [45] Lebensohn RA. *Acta Mater* 2001;49:2723–37.
- [46] Lebensohn RA, Castelnau O, Brenner R, Gilormini P. *Int J Solids Struct* 2005;42:5441–59.
- [47] Dykhne AM. *Sov Phys JETP* 1970;32:63–5.
- [48] Lurie KA, Cherkaev AV. *J Optimiz Theory Appl*. 1984;42:305–16.
- [49] Moulinec H, Suquet P. *Eur J Mech. A Solids* 2003;22:751–70.
- [50] Hershey AV. *J Appl Mech* 1954;21:236–40.
- [51] Kröner E. *J Phys F Metal Phys* 1978;8:2261–7.
- [52] Willis JR. *J Mech Phys Solids* 1977;25:185–202.
- [53] Eshelby JD. *Proc R Soc Lond* 1957;A241:376–96.
- [54] Hill R. *J Mech Phys Solids* 1965;13:89–101.